*Desalination and Water Treatment*
www.deswater.com
doi: 10.1080/19443994.2014.920731

55 (2015) 522–531
June

Taylor & Francis
Taylor & Francis Group

# Adsorptive removal of p-nitrophenol on microporous activated carbon by $FeCl_3$ activation: equilibrium and kinetics studies

Muthanna J. Ahmed[a,b,*], Samar K. Theydan[b]

[a]*Faculty of Engineering and Built Environment, Department of Chemical and Process Engineering, Universiti Kebangsaan Malaysia, Bangi 43600, Selangor, Malaysia, Tel. +60 129177261; Fax: +60 129177264; email: muthanna.ja@gmail.com*
[b]*Department of Chemical Engineering, University of Baghdad, Baghdad, Iraq, email: samarkarim26@yahoo.com*

Received 22 November 2013; Accepted 23 April 2014

## ABSTRACT

Microporous activated carbon from biomass wastes, date pits, has been utilized as adsorbent for removal of p-nitrophenol (PNPh) from aqueous solutions. The chemical activation with $FeCl_3$ was adopted for preparation and the characteristics of prepared carbon (FAC) represented by iodine number, surface area, micropores volume, and mesopores volume were 761.40 mg/g, 780.06 $m^2/g$, 0.468 $cm^3/g$, and 0.105 $cm^3/g$, respectively. The effect of variables represented by pH, adsorbent dose, contact time, and initial concentration on efficiency of FAC for PNPh removal was studied. Maximum removal efficiency of 94% was obtained at best conditions. Equilibrium adsorption data were analyzed by the Langmuir, Freundlich, and Sips isotherm models. The results showed that the best fit was achieved with the Sips isotherm equation, giving a maximum PNPh adsorption capacity of 184.86 mg/g. The adsorption kinetic data were well described by the pseudo-second-order model and the analysis of data showed that intraparticle diffusion cannot be considered as the rate-limiting step.

*Keywords:* Activated carbon; Date pits; p-Nitrophenol; Adsorption isotherm; Kinetics

## 1. Introduction

The complete removal of phenols from wastewaters, or in some cases, reduction in their concentrations to an acceptable level has become a major challenge, where such pollutants pose serious hazards to aquatic organisms [1]. The high persistence, non-biodegradability, and high toxicity of p-nitrophenol (PNPh) make it as one of the most hazardous polluting phenols to the environment. It can enter the human body through all routes and its toxic action is much like that of aniline [2]. PNPh aids the conversion of hemoglobin to methemoglobin, which is caused by the oxidation of iron(II) to iron(III) with the result that the hemoglobin can no longer transport oxygen in the body [3].

Several ways have been developed to remove phenols from wastewaters, including electrochemical oxidation, coagulation, solvent extraction, membrane separation, and photo catalytic degradation [4–8]. Among these techniques, adsorption using activated carbon is the most favorable method due to its capability for efficient adsorption of a broad range of phenols [9]. However, commercially available activated carbons are still considered as expensive materials for many countries due to the use of non-renewable and

---

*Corresponding author.

relatively expensive raw materials such as coal [10]. Therefore, in recent years, this has prompted a growing research interest in the production of activated carbons from renewable and cheaper precursors, which are mainly industrial and agricultural by-products [11].

Date pits as a raw material for the production of activated carbon can be considered as one of the best candidates among the agricultural wastes because it is cheap and quite abundant, especially in Mediterranean countries. Iraq is one of the largest date producing countries in the world. The number of date palm tree is estimated to be more than 21 million with an annual production of about 400,000 tons of the fruit. About 14% of the fruit is waste material in the form of seeds. Such a waste stream from the palm syrup factories has been harmful to the environment. Hence, from an economical consideration, its utilization is desirable to be used as a good precursor for activated carbon [12].

Physical and chemical activations are the common methods for production of activated carbon. Physical activation involves carbonization or pyrolysis of the carbonaceous materials at high temperatures (500–900˚C) in an inert atmosphere in order to eliminate the maximum of oxygen and hydrogen elements, followed by thermal activation at the same temperatures for pyrolysis or at a high temperature in the presence of oxidizing gas such as steam, air, and carbon dioxide [13]. By chemical activation, it is possible to prepare activated carbon in only one step. Pyrolysis and activation are carried out simultaneously in the presence of dehydrating agents such as $ZnCl_2$, $H_3PO_4$, and KCl [14].

Many studies have been done to remove PNPh from aqueous solutions using activated carbon prepared from different waste biomasses such as cane pith, apricots stones, coca shell, tea waste, kenaf natural fibers, and jute stick [15–20]. The smaller size of ferric cation enables ferric chloride to produce activated carbons with smaller pore sizes upon their activation, which will be more effective for removal of phenolic compounds with molecular diameters in the range of micropores content [21]. This work represents the first application of prepared activated carbon (FAC) as adsorbent for removal of PNPh from aqueous solutions. The equilibrium and kinetic data of the adsorption process are also studied to understand the adsorption mechanism.

## 2. Materials and methods

### 2.1. Materials

Date pits were used as precursor in the preparation of activated carbon. The pits as received were first washed with water to get rid of impurities, dried at 110˚C for 24 h, crushed using disk mill, and sieved. Fraction with average particle size of 2 mm was selected for the preparation. Ferric chloride (purchased from Scharlau company) of purity 99.9% was used as chemical reagent for activation of date pits. PNPh (supplied by BDH chemicals Ltd company) of purity higher than 99% was used as an adsorbate. All other chemical used such as hydrochloric acid, sodium thiosulfate, and iodine were of analytical grades.

### 2.2. Preparation and characterization of activated carbon

Ten grams of dried pits were well mixed with 100 mL of $FeCl_3$ solution at a concentration of 15 wt% for 24 h at 25 ± 2˚C. The impregnated samples were next dried at 110˚C until completely dried and stored in a desiccator. For the carbonization of dried impregnated samples, a stainless steel reactor (2.5 cm diameter × 10 cm length) was used. The reactor was sealed at one end and the other end had a removable cover with 2-mm hole at the center to allow the pyrolysis gases to escape. The reactor was placed in a furnace and heated at a constant rate of 10˚C/min and held at an activation temperature of 700˚C for an activation time of 1 h. At the end of activation time, the carbonized samples were withdrawn from the furnace and allowed to cool. Then, the samples were soaked with 0.1 M HCl solution, such that the liquid-to-solid ratio was 10 ml/g. The mixtures were left overnight at room temperature, and then filtered and subsequently the samples were repeatedly washed with distilled water until the pH of filtrate reached 6.5–7. After that, the samples were dried at 110˚C for 24 h. Finally, the samples were stored in tightly closed bottles.

The characteristics of FAC represented by pH value, moisture and ash contents, iodine number, surface area, micropores volume, mesopores volume, and pore size distribution were determined. The pH value of prepared activated carbon was determined by immersing 1 g sample in 100 mL deionized water and stirring at 150 rpm for 1 h and the pH of slurry was taken [22]. Moisture content was determined using oven drying method [23]. Ash content and iodine number, which is a measure of micropores content (0–20 Å), were determined by standard methods [24,25]. Surface area was determined from the application of Brunauer, Emmett and Teller (BET) equation to the adsorption–desorption isotherm of $N_2$ at 77 K [26]. Micropores volume was determined by applying the Dubinin–Radushkevich equation. The mesopores volume was determined using Barrett-Joyner-Halenda desorption branch [27] and the pore size distribution was determined from the density functional theory

[28]. NOVAWin2 data analysis software was used to perform these calculations [29]. The morphology of prepared activated and raw material was examined by scanning electron microscopy (SEM) (300 K Pixel CMOS, China).

### 2.3. Adsorptive removal

The ability of FAC to remove PNPh from aqueous solutions was determined under batch mode conditions. 50 ml samples of PNPh solutions with different initial concentrations (50–250 mg/L) and different pH (2–12) were mixed with FAC of particle size less than 250 μm at different adsorbent dose (0.2–1.8 g/L). The mixtures were added to 100-mL Erlenmeyer flasks, and the flasks were shaken at 120 rpm and 25 ± 2˚C for different contact time (0–120 min). At the end of contact time, the samples were filtered and the residual concentrations of PNPh in the filtrate were analyzed by a UV–Visible Spectrophotometer (Shimadzu UV-160A) at $\lambda_{\max}$ value of 400 nm. For all the experimental work, each experiment has been repeated twice and the adopted experimental concentration is the average of two readings. The best values of pH and contact time were determined by checking the effect of these variables on removal efficiency (%) of FAC to remove PNPh.

### 2.4. Adsorption isotherms

The maximum adsorption capacity of FAC for PNPh was determined by performing adsorption tests in a set of 100-mL Erlenmeyer flasks where 50 mL of PNPh solutions with initial concentrations of 50–250 mg/L were placed in these flasks. Then, the flasks were placed in an orbital shaker at 120 rpm and 25 ± 2˚C. Other operating parameters such as activated carbon dose, pH, and contact time were kept constant at their best values, which gave maximum removal efficiency as determined in adsorptive removal section. The concentrations of PNPh solutions were similarly measured and the amount of adsorption at equilibrium, $q_e$ (mg/g), was calculated using the following equation:

$$q_e = \frac{(C_0 - C_e)V}{W} \tag{1}$$

where $C_0$ and $C_e$ (mg/L) are the initial and equilibrium concentrations of PNPh solution, respectively, $V$ (L) is the volume of solution, and $W$ (g) is the weight of activated carbon used.

Three famous isotherm equations, namely the Langmuir, Freundlich, and Sips [30–32], were applied to fit the experimental isotherm data of PNPh adsorption on FAC. These equations can be written as:

$$\text{Langmuir isotherm} \qquad q_e = \frac{q_L K_L C_e}{1 + K_L C_e} \tag{2}$$

$$\text{Freundlich isotherm} \qquad q_e = K_F C_e^{1/n} \tag{3}$$

$$\text{Sips isotherm} \qquad q_e = \frac{q_S K_S C_e^{1/m}}{1 + K_S C_e^{1/m}} \tag{4}$$

where $q_L$ (mg/g) is the maximum adsorption capacity of FAC, $K_L$ (L/mg) is the Langmuir constant related to rate of adsorption, $K_F$ ((mg/g) (L/mg)$^{1/n}$) and $n$ are Freundlich constants, which give a measure of adsorption capacity and adsorption intensity, respectively, $q_S$ (mg/g) is the Sips maximum uptake of PNPh per unit mass of date stoned, $K_S$ (L/mg)$^{1/m}$ is Sips constant related to energy of adsorption, and parameter $m$ could be regarded as the Sips parameter characterizing the system heterogeneity. Least-squares regression program based on Hooke–Jeeves and Gauss–Newton method was used to analyze experimental data [33]. This program gave the parameters of each equation and the agreement between experimental and calculated data in terms of correlation coefficient $R^2$. The applicability of the isotherm models to describe the adsorption process was further validated by the normalized standard deviation, $\Delta q$ (%), which is defined as:

$$\Delta q\,(\%) = 100\sqrt{\frac{\sum[(q_{\exp} - q_{\text{cal}})/q_{\exp}]^2}{N - 1}} \tag{5}$$

where $N$ is the number of data points, $q_{\exp}$ and $q_{\text{cal}}$ (mg/g) are the experimental and calculated adsorption capacities, respectively.

### 2.5. Adsorption kinetics

The procedure used for kinetic tests was identical to that used for equilibrium experiments at best conditions. The aqueous samples were taken at preset time intervals, and the concentrations of PNPh were similarly measured. The adsorbed amount of PNPh at time $t$, $q_t$ (mg/g), was calculated depending on the concentration of PNPh at time $t$ using Eq. (1). Pseudo-first-order model, pseudo-second-order model, and intraparticle diffusion model [34–36] were used to analyze the kinetic data. These models can be expressed as:

Pseudo-first-order model $$\ln(q_t - q_e) = \ln(q_e) - K_1 t \quad (6)$$

Pseudo-second-order model $$\frac{t}{q_t} = \frac{1}{K_2 {q_e}^2} + \frac{t}{q_e} \quad (7)$$

Intraparticle diffusion model $$q_t = K_3 t^{1/2} + \mathrm{C} \quad (8)$$

where $q_e$ and $q_t$ (mg/g) are the uptake of PNPh at equilibrium and at time $t$ (min), respectively, $K_1$ (1/min) is the adsorption rate constant, $K_2$ (g/mg min) is the rate constant of second-order equation, $K_3$ (mg/g min$^{1/2}$) is the intraparticle diffusion rate constant, and $C$ (mg/g) is a constant that gives an idea about the thickness of the boundary layer. Besides the value of $R^2$, the normalized standard deviation, $\Delta q$ (%), calculated by Eq. (6) was also adopted to show the applicability of kinetics models to represent data.

## 3. Results and discussion

### 3.1. Characterization of prepared activated carbon

The ash and moisture contents of FAC were 6.62 and 12.54%, respectively. The iodine number in this study (761.40 mg/g) is greater than that obtained by Haimour and Emeish [37], 495 mg/g, for carbon prepared from date stones using $H_3PO_4$ activator. This indicates the ability of $FeCl_3$ to produce carbon structure with more micropores content as compared to that obtained using $H_3PO_4$. The structural characteristics of FAC have been compared with those for carbons prepared from date pits [38–42] by different activators (Table 1). In this study, the surface area of FAC (780.06 m$^2$/g) is higher than that reported by Hameed et al. [39] who showed that the surface area of activated carbon prepared by chemical activation of date stones with potassium hydroxide was 763.40 m$^2$/g. This may be due to smaller ionic radius of $Fe^{3+}$ ions (55 pm), which enable the formation of activated carbon with high total pore volume of 0.573 cm$^3$/g, compared to 0.424 cm$^3$/g using KOH, which has higher ionic radius for $K^{1+}$ (138 pm).

Fig. 1 shows the SEM images for the date pits and prepared activated carbons. As shown in Fig. 1(a), the surface of date pits is very smooth and there are very little pores on it which related to the smooth nature of date pit surface. After $FeCl_3$ activation, the surface of activated carbon becomes rough and many pores appear on it, (Fig. 1(b)). Also the formation of cavities, which provide channels for the PNPh molecules to access the micropores and mesopores inside the carbon particle, can be seen from Fig. 1(b). Fig. 2 displays the isotherms of $N_2$ adsorption (Fig. 2(a)) and pore size distribution (Fig. 2(b)) for the activated carbons prepared from date pits. It can be seen from Fig. 2(a) that the isotherm presents a high adsorption at low relative pressure, characteristics of microporous materials, where the adsorption branch resembles that of a type I isotherm in the international union of pure and applied chemistry (IUPAC) classification. From this figure, it can be also concluded that the isotherm displayed a small hysteresis loop, indicating the presence of very small mesopores volume. Fig. 2(b) presents the pore size distribution for the activated carbons made in this study. This figure shows that the pore structure consists basically of micropores, which are mainly defined by IUPAC as pores smaller than 20 Å in diameter. This can also be concluded from the results of Table 1, which show that $FeCl_3$ activation produced carbon structure with a highest micropores volume of 0.468 cm$^3$/g compared with those produced by $ZnCl_3$ and KOH activation. This may be related to smaller ionic radius of $Fe^{3+}$ ions (55 pm) compared with those of $Zn^{2+}$ (74 pm) and $K^{1+}$ (138 pm), which enables $FeCl_3$ to develop more micropores. Hence, it is interesting to observe that prepared activated carbon by ferric chloride activation showed the formation of carbon structure with high micropores content and better defined pores centered at approximately 8 Å (Fig. 2(b)), which are preferred for adsorption of phenols.

Table 1
Comparison of structural characteristics of date pits-carbon prepared by various activators

| Activator | Time (h) | Temp (˚C) | Conc. (g/g),(cc/min) | $S_{BET}$ (m$^2$/g) | $V_{mic}$ (cm$^3$/g) | $V_{mes}$ (cm$^3$/g) | Porous structure | Ref. |
|---|---|---|---|---|---|---|---|---|
| $FeCl_3$ | 1 | 700 | 1.50 | 780.06 | 0.468 | 0.105 | Microporous | This work |
| $ZnCl_2$ | 3 | 700 | 0.50 | 951.0 | 0.355 | 0.101 | Microporous | [37] |
| KOH | 2 | 700 | 3.00 | 763.4 | 0.215 | 0.209 | Microporous | [38] |
| $H_3PO_4$ | 1 | 400 | 3.00 | 725.0 | 0.391 | 0.869 | Mesoporous | [39] |
| $CO_2$ | 1 | 900 | 250 | 604.0 | 0.290 | 0.050 | Microporous | [40] |
| Steam | 4 | 700 | 150 | 438.0 | 0.126 | 0.096 | Microporous | [41] |

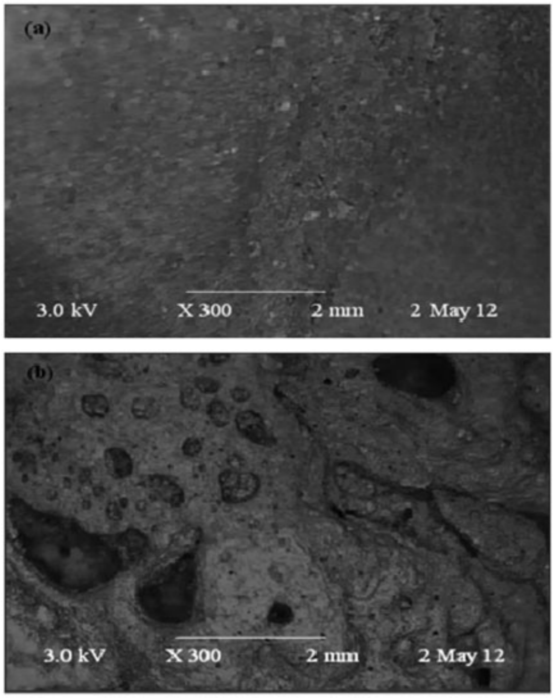

Fig. 1. SEM micrographs (300×) of date pits (a) and FAC (b).

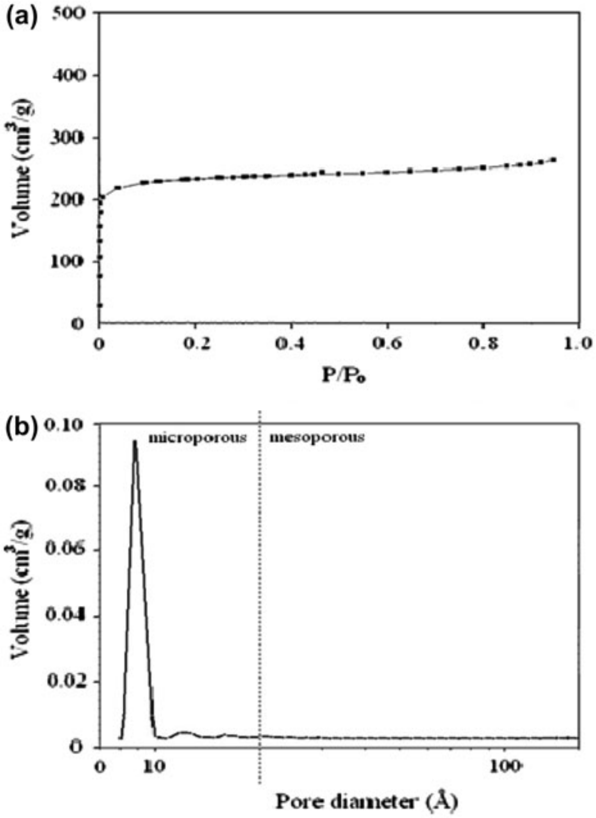

Fig. 2. Isotherms of $N_2$ adsorption–desorption (a) and pore size distribution (b) for FAC.

## 3.2. Adsorptive removal

The effect of pH, adsorbent dose, contact time, and initial concentration on removal efficiency is shown in Fig. 3.

### 3.2.1. Effect of pH

The effect of pH on the efficiency of FAC for removal of PNPh at different dose and 50 mg/L initial concentration can be shown in Fig. 3(a). The pH value is one of the key factors that control the adsorption process, because it influences the electrostatic interaction between the adsorbent and the adsorbate. It is clear from Fig. 3 that the removal efficiency increases with pH up to a value of 5, and thereafter it decreases. An increase in pH from 2 to 5 at 1.0 g/L dose and 50 mg/L initial PNPh concentration leads to an increase in removal efficiency from 82 to 94%. Therefore, the value of 5 is considered to be the best pH for removal of PNPh. Similar results were reported by Petrova et al. [9] who found that the best uptake for PNPh on activated carbon from coal tar pitch was at pH value of 5.6. In this study, prepared activated carbon FAC has a pH value of 6.5 as determined from Section 2.2, which revealed that its structure has a high content of acidic groups. At pH value above 5, the surface of activated carbon being negatively charged is causing a fall in removal efficiency, which is related to the repulsive interactions that appear between the anionic form of the adsorbates and the negative charges on the carbon surfaces, so that the amounts of PNPh adsorbed begin to decrease [43]. Fig. 3(a) also shows that the removal efficiency increases with increasing adsorbent dose up to a certain value of 1 g/L and then there is no further considerable increase in removal efficiency. An increase in adsorbent dose from 0.2 to 1.0 g/L at 5 pH value and 50 mg/L initial PNPh concentration leads to an increase in removal efficiency from 71.91 to 94%. Therefore, the value of 1 g/L can be considered as the best adsorbent dose that gives maximum removal efficiency.

### 3.2.2. Effect of contact time

The effect of contact time on removal efficiency for PNPh at different initial PNPh concentrations is shown in Fig. 3(b). It can be seen from this figure that

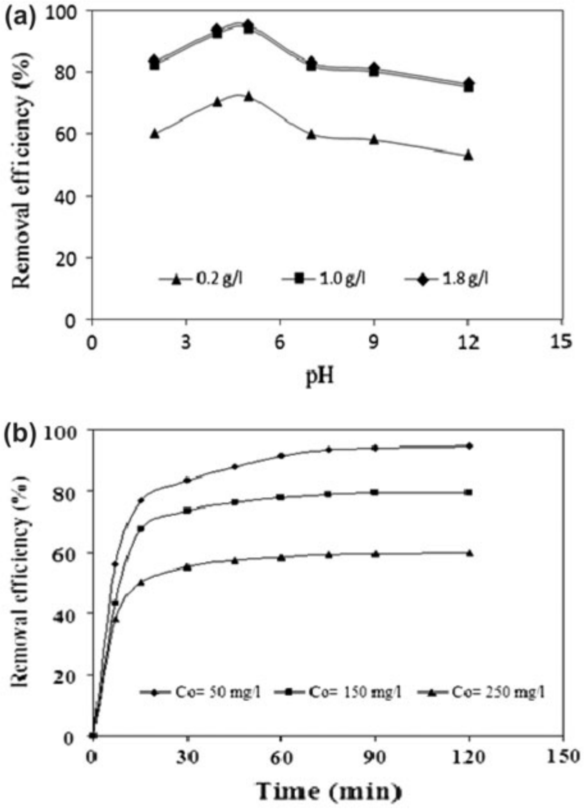

Fig. 3. Effect of pH at 50 mg/L and 90 min (a) and time at pH of 5 and 1 g/L (b) on removal efficiency.

the removal efficiency increases with the increase of contact time, and the adsorption reached equilibrium in about 90 min. For the studied range of initial PNPh concentration (50–250 mg/L), a maximum removal efficiency of 94% is obtained at 50 mg/L initial PNPh concentration. This figure also shows that rapid increase in removal efficiency is achieved during the first 25 min. The fast adsorption at the initial stage may be due to the higher driving force making fast transfer of PNPh ions to the surface of FAC particles and the availability of the uncovered surface area and the remaining active sites on the adsorbent [44]. This figure also shows that the removal efficiency decreased with increasing initial PNPh concentration. The increase in initial concentration from 50 to 250 mg/g leads to a decrease in removal efficiency from 94 to 59.64%, which is equivalent to an increase in adsorption capacity from 47 to 149.11 mg/g. This is because at lower initial PNPh concentration, the ratio of surface active sites to the total adsorbate molecules in the solution is high and hence, all adsorbate molecules may interact with the FAC and be removed from the solution [45].

### 3.3. Adsorption isotherms

According to the above discussion, the operating conditions, which give maximum removal efficiency for PNPh, were chosen as 5 pH value, 1 g/L adsorbent dose, and 90 min contact time.

The experimental equilibrium data for PNPh adsorption on FAC at optimum conditions, calculated from Eq. (1), are fitted with Langmuir, Freundlich, and Sips isotherms, Eqs. (2)–(4), and presented in Fig. 4. The calculated constants of the three isotherm equations along with $R^2$ values are presented in Table 2. This table shows that the three models correlate experimental data with $R^2$ values in the order of Sips > Langmuir > Freundlich. Also, the results of this table show that the deviation between the theoretical and experimental values $\Delta q$ (%) for the three models is in the order of Sips < Langmuir < Freundlich. The results revealed that the equilibrium data are fitted by the three-parameter model rather than the two-parameter models. The successful prediction of PNPh adsorption isotherm data using three-parameter isotherm has also been reported by Ahmaruzzaman and Sharma [46] on activated carbon, which may be due to the ability of three-parameter isotherms to predict wide adsorbate concentration ranges as compared to Langmuir and Freundlich isotherms. The favorable behavior for adsorption of PNPh onto prepared carbon from date pits can be concluded from the value of $1/n$, which is less than unity (0.290) for Freundlich isotherm fitting. The Langmuir model fitted the experimental data better than Freundlich model, indicating that the adsorption of PNPh onto FAC tended to monolayer adsorption. According to Sips isotherm fitting, the maximum adsorption capacity of PNPh is 184.86 mg/g. This value has been compared with those of carbons from other precursors (Table 3). It

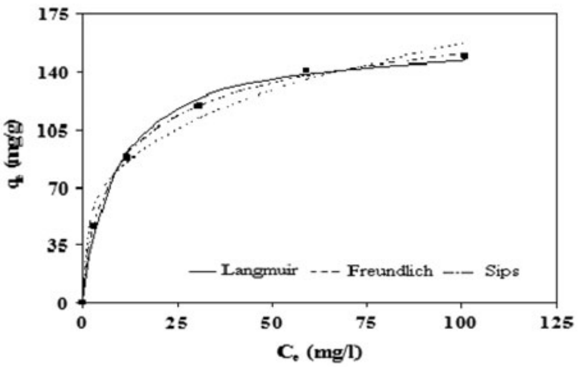

Fig. 4. Adsorption isotherm of PNPh on FAC at 25 ± 2°C (pH= 5, time= 90 min).

Table 2
Adsorption isotherm parameters at 25 ± 2˚C, pH = 5, and 90 min

| Isotherm | Parameter | Value |
|---|---|---|
| Langmuir | $q_m$ (mg/g) | 159.84 |
| | $K_L$ (L/mg) | 0.112 |
| | $R^2$ | 0.9946 |
| | $\Delta q$ (%) | 7.039 |
| Freundlich | $K_F$ ((mg/g) (L/mg)$^{1/n}$) | 41.35 |
| | $1/n$ | 0.290 |
| | $R^2$ | 0.9839 |
| | $\Delta q$ (%) | 10.969 |
| Sips | $q_S$ (mg/g) | 184.86 |
| | $K_S$ ((L/mg)$^{1/m}$) | 0.149 |
| | $m$ | 1.365 |
| | $R^2$ | 0.9993 |
| | $\Delta q$ (%) | 1.851 |

can be seen that the prepared activated carbon is more effective for this purpose.

### 3.4. Adsorption kinetics

The experimental kinetic data for PNPh adsorption on FAC at best conditions are presented in Fig. 3(b), which shows that the increase in initial concentration from 50 to 250 mg/g leads to a decrease in removal efficiency from 94 to 59.64%, which is equivalent to an increase in adsorption capacity from 47 to a maximum of 149.11 mg/g at equilibrium contact time of 90 min. These experimental data are fitted with pseudo-first-order, pseudo-second-order, and intraparticle diffusion models, Eqs. (6)–(8). The calculated constants of the three kinetics models along with $R^2$ and $\Delta q$ values at three different initial PNPh concentrations are presented in Table 4. The results of this table show that pseudo-first-order equation is of low $R^2$ values. Moreover, this table shows a large difference between the experimental and calculated adsorption capacity, indicating a poor pseudo-first-order fit to the experimental data. High $R^2$ values are obtained for the linear plot of $t/q_t$ vs. $t$ (Fig. 5) for pseudo-second-order equation, as shown in Table 4. This table shows that the pseudo-second-order kinetic model correlates experimental data with $R^2$ values of 0.9996, 0.9999, and 0.9999 for initial PNPh concentrations of 50, 150, and 250 mg/L, respectively. It can be seen that the pseudo-second-order kinetic model better represented the adsorption kinetics with lowest $\Delta q$ values that ranged between 0.423 and 0.659% for initial PNPh concentrations ranging from 50 to 250 mg/L (Table 4). This suggests that the adsorption of PNPh on FAC follows second-order kinetics. A similar result was reported for the adsorption of p-nitrophenol on jute stick-based activated carbon [20]. Fig. 5 also shows that the slope of linear plot decreases from 0.02 to 0.006 with increasing initial PNPh concentration from 50 to 250 mg/g, as concluded from results of Table 4. The reason for this behavior can be attributed to the low competition for the sorption surface sites at low concentration, which leads to lower sorption rates, where the values of rate constant $K_2$ decreases from 0.0038 to 0.0018 (g/mg min) with increasing initial PNPh concentration from 50 to 250 mg/g. Intraparticle diffusion model is widely used to predict the rate-controlling step, which is mainly depends on either surface or pore diffusion. $R^2$ values (Table 4) for this model were lower compared with those of pseudo-first-order and pseudo-second-order models. Also, there is high deviation between the theoretical and experimental values $\Delta q$ (%).This indicates that this intraparticle diffusion model cannot fit properly the experimental kinetic data for PNPh adsorption on FAC, which reveals that intraparticle diffusion cannot be considered as the rate-limiting step.

Table 3
Comparison of PNPh maximum capacities onto activated carbon prepared from various wastes

| Precursor | Activator | $T$ (K) | pH | $t$ (h) | Dose (g/L) | $q_{max}$ (mg/g) | Ref. |
|---|---|---|---|---|---|---|---|
| Date pits | $FeCl_3$ | 303 | 5.0 | 1.5 | 1.0 | 184.86 | This study |
| Cane pith | KOH | 303 | 7.0 | 72 | 0.5 | 347.78 | [15] |
| Apricot stones | steam | 298 | 7.0 | 2 | 2.0 | 179.00 | [16] |
| Coca shell | $CO_2$ | 303 | 7.0 | 0.5 | 4.0 | 166.67 | [17] |
| Tea waste | $H_3PO_4$ | 298 | 7.12 | 24 | 10 | 142.85 | [18] |
| Kenaf fibers | $K_2HPO_4$ | 299 | 6.0 | 72 | 1.0 | 136.99 | [19] |
| Jute stick | $H_3PO_4$ | 298 | 7.0 | 24 | 10 | 31.55 | [20] |

Table 4
Adsorption kinetics parameters at 25 ± 2°C, pH = 5, dose 1 g/L

| $C_0$ (mg/L) | $q_{e,exp}$ (mg/g) | $q_{e,cal}$ (mg/g) | $K_1$ (1/min) | $R^2$ | $\Delta q$ (%) |
|---|---|---|---|---|---|
| Pseudo-first order model | | | | | |
| 50 | 47.90 | 3.349 | 0.0327 | 0.9939 | 0.648 |
| 150 | 121.44 | 4.312 | 0.0292 | 0.9917 | 0.832 |
| 250 | 152.02 | 4.699 | 0.0291 | 0.9856 | 1.170 |
| Pseudo-second order model | | | | | |
| | $q_{e,exp}$ (mg/g) | $q_{e,cal}$ (mg/g) | $K_2$ (g/mg min) | | |
| 50 | 47.90 | 49.76 | 0.0038 | 0.9996 | 0.423 |
| 150 | 121.44 | 123.98 | 0.0022 | 0.9999 | 0.659 |
| 250 | 152.02 | 155.12 | 0.0018 | 0.9999 | 0.429 |
| Intraparticle diffusion model | | | | | |
| | $q_{e,exp}$ (mg/g) | $C$ (mg/g) | $K_3$ (mg/g min$^{1/2}$) | | |
| 50 | 47.90 | 32.89 | 1.572 | 0.9722 | 1.241 |
| 150 | 121.44 | 93.64 | 2.845 | 0.9599 | 1.829 |
| 250 | 152.02 | 120.99 | 3.140 | 0.9515 | 2.579 |

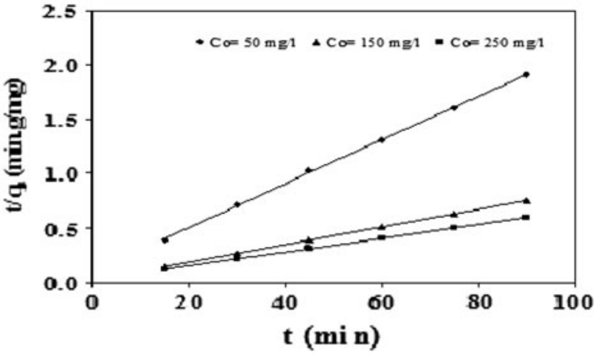

Fig. 5. Pseudo-second-order kinetics model (b) at pH 5 and dose 1 g/L.

## 4. Conclusions

Biomass wastes, date pits, have been utilized as precursors for activated carbon using ferric chloride activation. Within the studied range of initial concentration for PNPh (50–250 mg/L) and constant conditions of 5 pH value, 1 g/L adsorbent dose, and 90-min contact time, the prepared carbon showed a maximum removal percentage of 94%, which is equivalent for adsorption capacity of 149.11 mg/g. Equilibrium adsorption data of PNPh onto FAC were well represented by Sips isotherm model with maximum adsorption capacity of 184.86 mg/g. The adsorption kinetic data were well described by the pseudo-second-order model. Surface area, micropores volume, and mesopores volume of FAC were 780.06 m$^2$/g, 0.468 cm$^3$/g, and 0.105 cm$^3$/g, respectively.

## Acknowledgments

We gratefully acknowledge University of Baghdad and Universiti Kebangsaan Malaysia for the assist and support of this work.

## References

[1] A. Zhang, N. Wang, J. Zhou, P. Jiang, G. Liu, Heterogeneous Fenton-like catalytic removal of p-nitrophenol in water using acid-activated fly ash, J. Hazard. Mater. 201–202 (2012) 68–73.

[2] A.E. Ofomaja, E.I. Unuabonah, Adsorption kinetics of 4-nitrophenol onto a cellulosic material, mansonia wood sawdust and multistage batch adsorption process optimization, Carbohy. Polym. 83 (2011) 1192–1200.

[3] S. Al-Asheh, F. Banat, A. Masad, Kinetics and equilibrium sorption studies of 4-nitrophenol on pyrolyzed and activated oil shale residue, Environ. Geol. 45 (2004) 1109–1117.

[4] K. Jüttner, U. Galla, H. Schmieder, Electrochemical approaches to environmental problems in the process industry, Electrochim. Acta 45 (2000) 2575–2594.

[5] M. Tomaszewska, S. Mozia, A.W. Morawski, Removal of organic matter by coagulation enhanced with adsorption on PAC, Desalination 161 (2004) 79–87.

[6] S. Shen, Z. Chang, H. Liu, Three-liquid-phase extraction systems for separation of phenol and p-nitrophenol from wastewater, Sep. Purif. Technol. 49 (2006) 217–222.

[7] P. Anitha, N. Kavitha, K. Palanivelu, Removal and recovery of p-nitrophenol from aqueous solution using natural solid triglycerides, Desalination 272 (2011) 196–200.

[8] N. Sona, T. Yamamoto, D. Yamamoto, M. Nakaiwa, Degradation of aqueous phenol by simultaneous use of ozone with silica-gel and zeolite, Chem. Eng. Process 46 (2007) 513–519.

[9] B. Petrova, B. Tsyntsarski, T. Budinova, N. Petrov, L.F. Velasco, C.O. Ania, Activated carbon from coal tar pitch and furfural for the removal of p-nitrophenol and m-aminophenol, Chem. Eng. J. 172 (2011) 102–108.

[10] M.J. Martin, A. Artola, M.D. Balaguer, M. Rigola, Activated carbons developed from surplus sewage sludge for the removal of dyes from dilute aqueous solutions, Chem. Eng. J. 94 (2003) 231–239.

[11] P. Sathishkumar, M. Arulkumar, T. Palvannan, Utilization of agro-industrial waste Jatropha curcas pods as an activated carbon for the adsorption of reactive dye Remazol Brilliant Blue R (RBBR), J. Clean. Prod. 22 (2012) 67–75.

[12] M.J. Ahmed, S.K. Theydan, Equilibrium isotherms, kinetics and thermodynamics studies of phenolic compounds adsorption on palm-tree fruit stones, Ecotoxicol. Environ. Saf. 84 (2012) 39–45.

[13] C. Bouchelta, M.S. Medjram, O. Bertrand, J. Bellat, Preparation and characterization of activated carbon from date stones by physical activation with steam, J. Anal. Appl. Pyrolysis 82 (2008) 70–77.

[14] R. Yavuz, H. Akyildiz, N. Karatepe, E. Çetinkaya, Influence of preparation conditions on porous structures of olive stone activated by $H_3PO_4$, Fuel Process. Technol. 91 (2010) 80–87.

[15] R.L. Tseng, S.K. Tseng, Characterization and use of high surface area activated carbons prepared from cane pith for liquid-phase adsorption, J. Hazard. Mater. 136 (2006) 671–680.

[16] B. Petrova, T. Budinova, B. Tsyntsarski, V. Kochkodan, Z. Shkavro, N. Petrov, Removal of aromatic hydrocarbons from water by activated carbon from apricot stones, Chem. Eng. J. 165 (2010) 258–264.

[17] F. Ahmad, W.M.A. Wan Daud, M.A. Ahmad, R. Radzi, Using Coca (Theobroma Cacao) shell-based activated carbon to remove 4-nitro phenol from aqueous solution: Kinetics and equilibrium studies, Chem. Eng. J. 1781 (2011) 461–467.

[18] M. Ahmaruzzaman, S.L. Gayatri, Activated tea waste as a potential low-cost adsorbent for the removal of p-Nitrophenol from wastewater, J. Chem. Eng. Data 55 (2010) 4614–4623.

[19] S. Aber, A. Khataee, M. Sheydaei, Optimization of activated carbon fiber preparation from kenaf using $K_2HPO_4$ as chemical activator for adsorption of phenolic compounds, Bioresour. Technol. 100 (2009) 6586–6591.

[20] M. Ahmaruzzaman, S.L. Laxmi Gayatri, Batch adsorption of 4-nitrophenol by acid activated jute stick char: Equilibrium, kinetic and thermodynamic studies, Chem. Eng. J. 158 (2010) 173–180.

[21] M.J. Ahmed, S.K. Theydan, Physical and chemical characteristics of activated carbon prepared by pyrolysis of chemically treated date stones and its ability to adsorb organics, Powder Technol. 229 (2012) 237–245.

[22] P.A. Egwaikhide, E.E. Akporhono, F.E. Okieimen, Utilization of coconut fibre carbon in the removal of soluble petroleum fraction polluted water, Int. J. Phys. Sci. 2 (2007) 047–049.

[23] F.A. Adekola, H.I. Adegoke, Adsorption of blue-dye on activated carbons produced from Rice Husk, Coconut Shell and Coconut Coir pitch, Ife J. Sci. 7 (1) (2005) 151–157.

[24] ASTM standard, Standard test method for total ash content of activated carbon, Designation D2866-94 (2000).

[25] Lubrizol standard test method, Iodine value, test procedure AATM 1112-01, October 16 (2006).

[26] S. Brunauer, P.H. Emmett, E. Teller, Adsorption of gases in multimolecular layers, JACS 60 (1938) 309–319.

[27] S.J. Gregg, K.S.W. Sing, Adsorption, surface area and porosity, Academic Press, London, 1966.

[28] C. Lastoskie, K.E. Gubbins, N. Quirke, Pore size distribution analysis of microporous carbons: a density functional theory approach, J. Phys. Chem. 97 (1993) 4786–4796.

[29] S. Lowell, J.E. Shields, M.A. Thomas, M. Thommes, Characterization of porous solids and powders: Surface area, pore size and density, Kluwer, Dordrecht, 2004.

[30] I. Langmuir, The adsorption of gases on plane surfaces of glass, mica and platinum, JACS 40 (1918) 1361–1403.

[31] H.M.F. Freundlich, Über die adsorption in lösungen, Z. Phys. Chem. 57 (1906) 385–470.

[32] R. Sips, On the structure of a catalyst surface, J. Chem. Phys. 16 (1948) 490–495.

[33] Statistica Release 7, copyright, softstat, Inc., 1984-2004.

[34] Y.S. Ho, Citation review of Lagergren kinetic rate equation on adsorption reactions, Scientometrics 59 (2004) 171–177.

[35] Y.S. Ho, G. Mckay, Pseudo-second order model for sorption processes, Process Biochem. 34 (1999) 451–465.

[36] W.J. Weber, J.C. Morris, Kinetics of adsorption on carbon from solution, J. Saint. Eng. Div. Am. Soc. Civil Eng. 89 (1963) 31–60.

[37] N.M. Haimour, S. Emeish, Utilization of date stones for production of activated carbon using phosphoric acid, Waste Manage. 26 (2006) 651–660.

[38] Y.A. Alhamed, Phenol removal using granular activated carbon from dates'stones, Bulg. Chem. Commun. 41 (2008) 26–35.

[39] B.H. Hameed, J.M. Salman, A.L. Ahmad, Adsorption isotherm and kinetic modeling of 2,4-D pesticide on activated carbon derived from date stones, J. Hazard. Mater. 163 (2009) 121–126.

[40] K.S.K. Reddy, A. Al Shoaibi, C. Srinivasakannan, A comparison of microstructure and adsorption characteristics of activated carbons by $CO_2$ and $H_3PO_4$ activation from date palm pits, New Carbon Mater. 27 (5) (2012) 344–351.

[41] M.L. Sekirifa, M. Hadj-Mahammed, S. Pallier, L. Baameur, D. Richard, A.H. Al-Dujaili, Preparation and characterization of an activated carbon from a date stones variety by physical activation with carbon dioxide, J. Anal. Appl. Pyrolysis 99 (2013) 155–160.

[42] C. Bouchelta, M.S. Medjram, M. Zoubida, F.A. Chekkat, N. Ramdane, J.-P. Bellat, Effects of pyrolysis conditions on the porous structure development of date pits activated carbon, J. Anal. Appl. Pyrolysis 94 (2012) 215–222.

[43] D. Tang, Z. Zheng, K. Lin, J. Luan, Adsorption of p-nitrophenol from aqueous solutions onto activated carbon fiber, J. Hazard. Mater. 143 (2007) 49–56.

[44] M.K. Aroua, S.P.P. Leong, L.Y. Teo, Chun Yang Yin, Real-time determination of kinetics of adsorption of lead(II) onto palm shell-based activated carbon using ion selective electrode, Bioresour. Technol. 99 (2008) 5786–5792.

[45] S.Z. Mohammadi, M.A. Karimi, D. Afzali, F. Mansouri, Removal of Pb(II) from aqueous solutions using activated carbon from sea-buckthorn stones by chemical activation, Desalination 262 (2010) 86–93.

[46] M. Ahmaruzzaman, D.K. Sharma, Adsorption of phenols from wastewater, J. Colloid Interface Sci. 287 (2005) 14–24.